Functionalized Carborane Complexes of the $[M(CO)_2(NO)]^{2+}$ Core (M = ^{99m}Tc, Re): A New Class of Organometallic Probes for Correlated *in Vitro* and *in Vivo* Imaging

Andrea F. Armstrong,[†] Julie M. Lebert,[‡] John D. Brennan,[‡] and John F. Valliant*[,†,§]

McMaster Institute for Applied Radiation Sciences, McMaster University, Chemical Biology Graduate Program, Department of Chemistry, McMaster University, and Departments of Chemistry and Medical Physics & Applied Radiation Sciences, McMaster University, Hamilton, Ontario, Canada, L8S 4M1

Received December 12, 2008

Functionalized carborane complexes of the $[M(CO)_2(NO)]^{2+}$ (M = Re, ^{99m}Tc) core have potential utility as matched pairs of probes for correlated optical (M = Re) and scintigraphic (M = ^{99m}Tc) imaging. A synthetic route to *closo*-rhenacarboranes of the type $[Re(CO)_2(NO)(RR'C_2B_9H_9)]$ in a manner suitable for the preparation of the radioactive technetium-99m analogues has been developed, resulting in the isolation of four novel metallacarboranes $[Re(CO)_2(NO)(RR'C_2B_9H_9)]$, which exhibit both 3,1,2 (**6a**: R = H, R′ = Bn) and 2,1,8 (**7a**: R = R′ = H; **8a**: R = H, R′ = Ph; **9a**: R = R′ = Bn) cage configurations. These complexes absorb strongly at 300−348 nm; **6a**−**9a** fluoresce weakly at ambient temperature following excitation at 300 nm (**7a**) or ∼340 nm (**6a**, **8a**/**9a**), with emission maxima ranging between 313 and 411 nm. A microwave-assisted approach was used to prepare radioactive $[^{99m}Tc(CO)_3]^+$-carborane complexes (**1b**−**4b**) at the tracer level. When an analogous aqueous nitrosation methodology was applied to generate dicarbonylnitroso-*closo*-technetacarboranes, the novel complexes **6b**, **8b**, and **9b** were isolated in good radiochemical yields (62−79%). In aqueous solutions, slow decomposition of **6b** and **8b**, but not **9b** was observed. To better understand this process, the radioactive $^{186/188}$Re analogue of **8a** was also prepared.

Introduction

Molecular imaging comprises a number of techniques that can be used to noninvasively visualize biological targets and processes *in vivo*.[1] Diagnostic radioimaging techniques such as single photon emission computed tomography (SPECT) play an increasingly important role in this field, particularly in the assessment of human disease.[2] The radioactive probes or "radiotracers" used with SPECT imaging generally consist of a radioisotope such as ^{99m}Tc linked to a targeting vector that directs the molecule to the selected biological target.[3]

For novel molecular imaging probes, it is essential to establish the mechanism of target binding and kinetics of uptake at the cellular level. This has prompted a search for new classes of synthons that can be used for both *in vivo* imaging studies and *in vitro* imaging (fluorescence microscopy) experiments to ensure good correlation between the two types of data. To facilitate these types of studies, we have previously developed bifunctional chelate complexes of the rhenium tricarbonyl core $[Re(CO)_3]^+$ that are luminescent and can thus be monitored *in vitro* by fluorescence microscopy, while their ^{99m}Tc analogues can be used for radioimaging (SPECT).[4,5] The utility of these compounds has provided an impetus for further work in this area, directed at the discovery of new classes of complementary fluorescent and radioactive probes to broaden the scope of this emerging field.[6−13]

* To whom correspondence should be addressed. Tel: +1-905-525-9140, ext. 22840. Fax: +1-905-522-7776. E-mail: valliant@mcmaster.ca.
[†] McMaster Institute for Applied Radiation Sciences.
[‡] Chemical Biology Graduate Program, Department of Chemistry.
[§] Departments of Chemistry and Medical Physics & Applied Radiation Sciences.

(1) For recent reviews of molecular imaging techniques and applications, see: (a) Yang, D. J.; Chanda, M.; Sims-Mourtada, J.; Azhdarinia, A.; Oh, C.-S.; Bryant, J.; Kim, E. E. *Mol. Imaging Rev.* **2008**, *4* (1), 46–50. (b) Ametamey, S. M.; Honer, M.; Schubiger, P. A. *Chem. Rev.* **2008**, *18* (5), 1501–1516. (c) He, J.; Van Brocklin, F.; Franc, B. L.; Seo, Y.; Jones, E. F. *Nanoscience* **2008**, *4* (1), 17–29. (d) Waters, E. A.; Wickline, S. A. *Basic Res. Cardiol.* **2008**, *103* (2), 114–121. (e) Jagannathan, N. R. *Curr. Sci.* **2007**, *92* (8), 1061–1070. (f) Dayton, P. A.; Rychak, J. J. *Front. Biosci.* **2007**, *12*, 5124–5142. (g) Sokolov, K.; Nida, D.; Descour, M.; Lacy, A.; Levy, M.; Hall, B.; Dharmawardhane, S.; Ellington, A; Korgel, B.; Richards-Kortum, R. *Adv. Cancer Res.* **2007**, *96*, 299–344. (h) Ruan, G.; Agrawal, A.; Smith, A. M.; Gao, X.; Nie, S. *Rev. Fluor.* **2006**, *3*, 181–193.

(2) See, for example: (a) Bailey, D. L., Meikle, S. R. *SPECT: Basic Science and Clinical Applications*; Springer Press, 2008. (b) Israel, O., Goldsmith, S. J., Eds. *Hybrid SPECT/CT Imaging in Clinical Practice*; Informa Healthcare, 2006.

(3) See, for example: (a) Mindt, T.; Struthers, H.; Garcia-Garayoa, E.; Desbouis, D.; Schibli, R. *Chimia* **2007**, *61* (11), 725–731. (b) Ferro-Flores, G.; Arteage de Murphy, C.; Melandez-Alafort, L. *Curr. Pharm. Anal.* **2006**, *2* (4), 339–352. (c) Perkins, A. C. *Biomed. Imaging Intervention J.* **2005**, *1* (2). (d) Liu, S. *Chem. Soc. Rev.* **2004**, *33* (7), 445–461.

(4) Stephenson, K. A.; Banerjee, S. R.; Besanger, T.; Sogbein, O. O.; Levadala, M. K.; McFarlane, N.; Lemon, J. A.; Boreham, D. R.; Maresca, K. P.; Brennan, J. D.; Babich, J. W.; Zubieta, J.; Valliant, J. F. *J. Am. Chem. Soc.* **2004**, *126* (28), 8598–8599.

(5) Schaffer, P.; Gleave, J. A.; Lemon, J. A.; Reid, L. C.; Pacey, L. K. K.; Farncombe, T. H.; Boreham, D. R.; Zubieta, J.; Babich, J. W.; Doering, L. C.; Valliant, J. F. *Nuc. Med. Biol.* **2008**, *35*, 159–169.

(6) Holland, J. P.; Barnard, P. J.; Bayly, S. R.; Betts, H. M.; Churchill, Dilworth, J. R.; Edge, R.; Green, J. C.; Hueting, R. *Eur. J. Inorg. Chem.* **2008**, 1985–1993.

(7) Pascu, S. I.; Waghorn, P. A.; Conry, T. D.; Lin, B.; Betts, H. M.; Dilworth, J. R.; Sim, R. B.; Churchill, G. C.; Aigbirhio, F. I.; Warren, J. E. *Dalton Trans.* **2008**, 2107–2110.

(8) Agorastos, N.; Borsig, L.; Renard, A.; Antoni, P.; Viola, G.; Spingler, B.; Kurz, P.; Alberto, R. *Chem.−Eur. J.* **2007**, *13*, 3842–3852.

(9) Pascu, S. I.; Waghorn, P. A.; Conry, T. D.; Lin, B.; Betts, H. M.; Dilworth, J. R.; Sim, R. B.; Churchill, G. C.; Pokrovska, T.; Christlieb, M.; Aigbirhio, F. I.; Warren, J. E. *Dalton Trans.* **2007**, 4988–4997.

(10) Wei, L.; Babich, J. W.; Ouellette, W.; Zubieta, J. *Inorg. Chem.* **2006**, *45* (7), 3057–3066.

10.1021/om8011807 CCC: $40.75
Publication on Web 04/21/2009

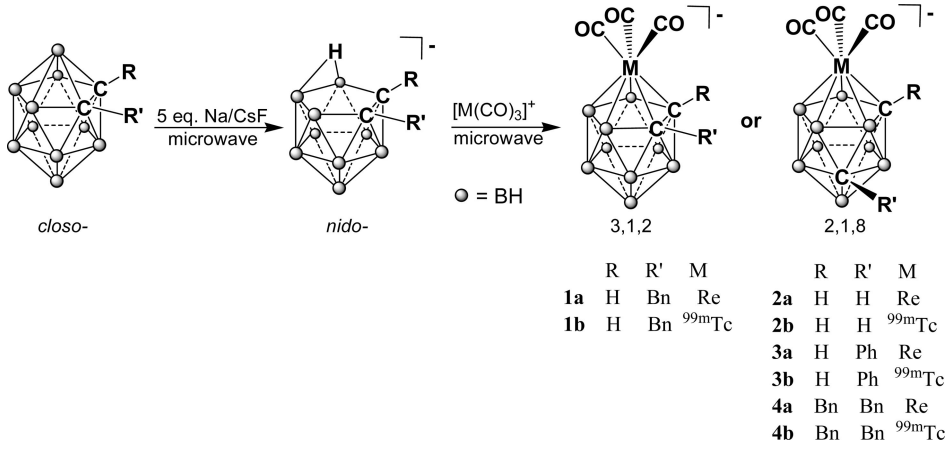

	R	R'	M
1a	H	Bn	Re
1b	H	Bn	^{99m}Tc

	R	R'	M
2a	H	H	Re
2b	H	H	^{99m}Tc
3a	H	Ph	Re
3b	H	Ph	^{99m}Tc
4a	Bn	Bn	Re
4b	Bn	Bn	^{99m}Tc

Figure 1. Synthesis of representative 3,1,2- and 2,1,8-metallacarboranes. Shaded circles represent BH units.

We have recently described a highly efficient synthetic route for the preparation of carborane complexes of rhenium via the microwave-assisted reaction of *fac*-$[Re(CO)_3(H_2O)_3]^+$ with functionalized *nido-ortho*-carboranes $[RR'C_2B_9H_{10}]^-$.[14] The resulting rhenacarboranes (Figure 1) were obtained as either the expected 3,1,2 species (**1a**) or as the isomeric 2,1,8 complexes (**2a**−**4a**) where one of the carbon atoms of the carborane cage has migrated out of the ligand−metal bonding face. Further investigation of the isomerization process[15] revealed the importance of both steric and electronic aspects of the cage substituents in determining whether conversion to the more thermally stable 2,1,8-rhenacarborane occurs. Regardless of the isomeric form, these complexes have several properties that render them suitable for use as radiopharmaceuticals, such as stability in aqueous media, low molecular weight, and synthetic versatility, which readily allows a targeting vector to be appended to the carborane cage. We have also demonstrated that this methodology can be translated to tracer level reactions with *fac*-$[^{99m}Tc(CO)_3(H_2O)_3]^+$.[14]

The synthesis of the closely related complex [3,3-$(CO)_2$-3-(NO)-3,1,2-*closo*-$ReC_2B_9H_{11}$] (**5**) has been reported in the literature,[16] and its electronic spectra and luminescence behavior have been described in detail.[17,18] These emissive properties indicate that functionalized carborane complexes of the *fac*-$[Re(CO)_2(NO)]^{2+}$ core may comprise a new class of organometallic probes that can be detected *in vitro* by fluorescence microscopy: the isostructural radioactive metallacarboranes could then serve as complementary radioimaging (^{99m}Tc) and radiotherapy ($^{186/188}$Re) agents. The structural similarity between the nitrosyl metallacarboranes and the $[Re(CO)_3]^+$ carborane complexes **1a**−**4a** suggests that they will retain many of the favorable properties of the latter species.

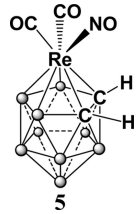

5

The general utility of these organometallic complexes for molecular imaging hinges upon the development of a method of preparing the targets rapidly, in high yields and in aqueous media. Aqueous nitrosations, as opposed to reactions conducted in organic solvents,[19−24] have now been explored for the simple inorganic salt *fac*-$[Re(CO)_3Br_3]^-$ of the rhenium tricarbonyl core,[25] but not for complexes containing organic ligands. Thus the objectives of this work were to develop a synthetic route to functionalized dicarbonyl nitrosyl rhenacarboranes, determine the fluorescence properties of these species, and then attempt to adapt this synthetic methodology to tracer level work with ^{99m}Tc to prepare the complementary radioimaging agents.

Experimental Section

Reagents and General Procedures. The *closo*-rhenacarboranes [Cs][**1a**−**4a**] were prepared according to the literature procedure,[15] substituting CsF in place of NaF. Nitrosonium sources $NaNO_2$ (98%, BDH), $[NO][BF_4]$ (95%, Aldrich), and $[NO][HSO_4]$ (40% w/v in H_2SO_4) were obtained from commercial suppliers and used without further purification. Deuterated solvents were obtained from Cambridge Isotope Laboratories. Aqueous tetraethylammonium phosphate (TEAP, pH 2.2), used as an HPLC solvent, was prepared by combining Et_3N (3.5 mL, 25 mmol) and H_3PO_4 (85%, 2.25 mL, 19.5 mmol) in HPLC grade H_2O (500 mL). Thin-layer chromatograms (Merck F_{254} silica gel on aluminum plates) were visualized using 0.1% $PdCl_2$ in 3 M $HCl_{(aq)}$ and UV light. Reverse phase (C18)

(11) Smithback, J. L.; Helms, J. B.; Schutte, E.; Woessner, S. M.; Sullivan, B. P. *Inorg. Chem.* **2006**, *45* (5), 2163–2174.

(12) Bullok, K. E.; Gammon, S. T.; Violini, S.; Prantner, A. M.; Villalobos, V. M.; Sharma, V.; Piwnica-Worms, D. *Mol. Imaging* **2006**, 1–15.

(13) Cowley, A. R.; Davis, J.; Dilworth, J. R.; Donnelley, P. S.; Dobson, R.; Nightingale, A.; Peach, J. M.; Shore, B.; Kerr, D.; Seymour, L. *Chem. Commun.* **2005**, 845–847.

(14) Green, A. E. C.; Causey, P. W.; Louie, A. S.; Armstrong, A. F.; Harrington, L. E.; Valliant, J. F. *Inorg. Chem. (Commun.)* **2006**, *45* (15), 5727–5729.

(15) Armstrong, A. F.; Valliant, J. F. *Inorg. Chem.* **2007**, *46* (6), 2148–2158.

(16) Ellis, D. E.; Jelliss, P. A.; Stone, F. G. A. *Chem. Commun.* **1999**, 2385–2386.

(17) Bitterwolf, T. E.; Scallorn, W. B.; Weiss, C. A.; Jelliss, P. A. *Organometallics* **2002**, *21* (9), 1856–1860.

(18) Fischer, M. J.; Jelliss, P. A.; Orlando, J. H.; Phifer, L. M.; Rath, N. P. *J. Lumin.* **2005**, *114*, 60–64.

(19) Rattat, D.; Verbruggen, A.; Schmalle, H.; Berke, H.; Alberto, R. *Tetrahedron Lett.* **2004**, *45*, 4089–4092.

(20) Rattat, D.; Schubiger, P. A.; Berke, H. G.; Schmalle, H.; Alberto, R. *Cancer Biother. Radiopharm.* **2001**, *16* (4), 339–343.

(21) Hund, H.-U.; Ruppli, U.; Berke, H. *Helv. Chim. Acta* **1993**, *76* (2), 963–975.

(22) Norton, J. R.; Dolcetti, G. *Inorg. Chem.* **1973**, *12* (2), 485–487.

(23) Uguagliati, P.; Zingales, F.; Trovati, A. *Inorg. Chem.* **1971**, *10* (3), 510–513.

(24) Uguagliati, P.; Zingales, F.; Trovati, A.; Cariati, F. *Inorg. Chem.* **1971**, *10* (3), 507–510.

(25) Schibli, R.; Marti, N.; Maurer, P.; Spingler, B.; Lehaire, M.-L.; Gramlich, V.; Barnes, C. L. *Inorg. Chem.* **2005**, *44*, 683–690.

solid phase extraction cartridges (1.6 mL) were obtained from Waters and flushed with water (10 mL), methanol (10 mL), and water (10 mL) again prior to use. Radiochemistry experiments were conducted in a licensed facility using appropriate shielding. Sodium pertechnetate [Na][$^{99m}TcO_4$] was obtained from a commercial $^{99}Mo/^{99m}Tc$ generator (BMS) and converted to $[^{99m}Tc(CO)_3(H_2O)_3]^+$ using a microwave-assisted approach.[26] $[^{186/188}ReO_4]^-$ was provided by the McMaster Nuclear Reactor; $[^{186/188}Re(CO)_3(H_2O)_3]^+$ was generated according to the literature procedure.[26]

Instrumentation. Nuclear magnetic resonance (NMR) spectra were acquired on a Bruker DRX-500 NMR spectrometer. ^1H NMR chemical shifts are reported in parts per million relative to tetramethylsilane referenced to residual proton signals of the deuterated solvent. ^{13}C NMR chemical shifts (in ppm) were referenced to the deuterated solvent signals, while $^{11}B(^1H)$ NMR spectra were referenced to an external standard of $[BF_3 \cdot OEt_2]$. Mass spectrometry analyses were provided by the McMaster Regional Centre for Mass Spectrometry using either a Waters Micromass Quattro Ultima Triple Quadrupole (electrospray ionization) or Waters Micromass GCT Time of Flight (chemical ionization) mass spectrometer. Microwave-assisted reactions were conducted in a Biotage Initiator 60 or Initiator 8 microwave. Automated reverse phase silica gel chromatography was accomplished using a Biotage SP4 automated purification system and a C18 column.

Optical Measurements. The solution absorption characteristics of **6a**−**9a** (500 μM in acetonitrile) were examined at 250−700 nm using a Cary 100 UV/vis instrument. Molar extinction coefficients were determined using Beer's law: all four compounds gave highly linear trends with $R^2 \geq 0.999$. The fluorescence emission spectra for compounds **6a**−**9a** in acetonitrile under N_2-equilibrated and air-equilibrated conditions were measured at 22 °C using a Jobin Yvon-SPEX Fluorolog-3 model 212 T-format spectrofluorimeter (ISA, Edison, NJ) with excitation at 250 nm, λ_{max}, and at the shoulder of λ_{max} (**6a**, 400 nm; **7a**, 340 nm; **8a**, 410 nm; **9a**, 405 nm). Spectra were corrected for solvent contributions. The Raman intensities of the sample and blank were matched to account for inner filter effects due to the large amount of analyte required to obtain usable emission spectra.

The quantum yield of **7a** was determined using a Cary Eclipse fluorescence spectrophotometer with POPOP in cyclohexane as the quantum yield reference. All solutions had optical densities of less than 0.05 to eliminate variation due to the inner filter effect. Fluorescence spectra were integrated using the Cary Eclipse software and corrected for solvent contributions.

The fluorescence lifetimes for both air-equilibrated and N_2-equilibrated samples of **7a** (25 μM) were assessed using time-correlated single-photon counting (TCSPC) on a IBH 5000U instrument. A pulsed ultraviolet light-emitting diode operating at 500 kHz with 1.3 ns pulse duration was used for excitation of **7a**. The fluorescence data were collected without excitation or emission polarizers in place; the excitation and emission monochromators were set to 350 and 420 nm, respectively, with a long pass filter (410 nm) in place. Decay data for **7a** were collected into 1024 channels and corrected with an instrument response function. The decay was fit to a triexponential decay model with $\chi^2 = 1.73$ (N_2-equilibrated) or $\chi^2 = 1.88$ (air-equilibrated). Time components and percent contribution for N_2-equilibrated sample: $\tau_1 = 4.6 \pm 0.2$ ns (71%); $\tau_2 = 16.8 \pm 0.08$ ns (29%); average lifetime = 8.1 ns. For air-equilibrated sample: $\tau_1 = 3.4 \pm 0.2$ ns (52%); $\tau_2 = 10.0 \pm 0.2$ ns (48%); average lifetime = 6.6 ns. The third lifetime component corresponded to scattering. Both solutions had absorbance values < 0.05 to eliminate the need for self-absorbance corrections.

High-Performance Liquid Chromatography (HPLC). Reverse phase high-performance liquid chromatography (HPLC) was conducted using a Varian Pro Star 330 PDA detector operating at $\lambda =$ 254 nm with a model 230 solvent delivery system and an in-line β-RAM Radio-HPLC detector (IN/US Systems, model 3). A Nucleosil analytical C18 column (4.6 mm × 10 cm) and a flow rate of 1.0 mL/min were employed. The following solvent gradients were used: Method A (solvent A = $TEAP_{(aq)}$, solvent B = MeOH) 0−3 min, 100% A; 3−6 min, 100% A to 75% A; 6−9 min, 75% A to 67% A; 9−20 min, 67% A to 0% A; 20−22 min,0% A; 22−25 min, 0% A to 100% A; 25−30 min, 100% A; Method B (solvent A = H_2O, solvent B = CH_3CN) 0−17 min, 85% B to 98% B; 17−20 min, 98% B.

Preparation of [3,3-$(CO)_2$-3-(NO)-1-(Bn)-3,1,2-*closo*-$ReC_2B_9H_{10}$] (6a). In a typical experiment, [Cs][**1a**] (208.4 mg, 0.3330 mmol) was dissolved in a mixture of CH_3CN/H_2O (3:1, 20 mL), resulting in a clear colorless solution. Aqueous $NaNO_2$ (0.646 mL, 23.0 mg, 0.333 mmol) and H_2SO_4 (2.0 M, 0.333 mL, 0.666 mmol) were then added at ambient temperature, and the reaction mixture became yellow instantaneously. After 2.5 h, second portions of both aqueous $NaNO_2$ (0.200 mL, 7.11 mg, 0.103 mmol) and H_2SO_4 (2.0 M, 0.100 mL, 0.200 mmol) were added and stirring was continued for an additional 18 h. The resulting bright yellow solution was combined with CH_2Cl_2 (40 mL) and washed with H_2O (1 × 30 mL). The organic layer was dried over Na_2SO_4 prior to removal of the solvent by rotary evaporation. The yellow residue was purified by automated reverse phase (C18) silica gel chromatography employing a gradient of 60−100% CH_3CN in H_2O, leaving **6a** as a bright yellow oil (111.2 mg, 67%). ^1H NMR (CD_2Cl_2, δ): 7.29 (m, 3 H, Ph), 7.14 (m, 2 H, Ph), 3.26 (s, 2 H, CH_2), 2.56 (s, 1H, CH). $^{11}B(^1H)$ NMR (CD_2Cl_2, δ): 1.6, (1 B), −3.5 (2 B), −6.7 (2 B), −9.9 (1 B), −11.2 (1 B), −15.3 (1 B), −15.8 (1 B). $^{13}C(^1H)$ NMR (CD_2Cl_2, δ): 189.4, 188.9, 138.3, 130.7, 128.7, 127.8, 66.1, 46.9, 43.1. IR (neat): 2574.8 (br, ν_{B-H}), 2082.9 ($\nu_{C=O}$), 2023.1 ($\nu_{C=O}$), 1772.4 cm^{-1} ($\nu_{N=O}$). TLC (10% CH_2Cl_2 in hexanes): $R_f = 0.20$. HPLC $t_R = 8.9$ min (method B). HRMS (CI^-) m/z for $C_{11}H_{17}NO_3B_9Re$: calcd 497.1604, obsd 497.1603 [M^+].

Preparation of [2,2-$(CO)_2$-2-(NO)-2,1,8-*closo*-$ReC_2B_9H_{11}$] (7a). Compound [Cs][**2a**] (104 mg, 0.194 mmol) was dissolved in a mixture of CH_3CN (15 mL) and H_2O (5 mL), forming a clear colorless solution. Aqueous solutions of $NaNO_2$ (0.40 mL, 13.9 mg, 0.202 mmol) and H_2SO_4 (6.0 M, 0.10 mL, 0.60 mmol) were added to the reaction mixture; after stirring for 60 min additional portions of $NaNO_2$ (0.20 mL, 6.95 mg, 0.101 mmol) and H_2SO_4 (6.0 M, 0.10 mL, 0.60 mmol) were added. After an additional 30 min the volatile component (CH_3CN) of the reaction solvent was removed from the bright yellow solution by rotary evaporation. The product was extracted into CH_2Cl_2 (25 mL) and washed with H_2O (25 mL); the organic phase was dried over Na_2SO_4 prior to removal of the solvent by rotary evaporation. The crude product (73.7 mg, 0.182 mmol, 94%) was loaded onto a reverse phase solid phase extraction cartridge; impurities were eluted with aqueous CH_3CN (75%, 5 mL) prior to elution of compound **7a** with neat CH_3CN. Following removal of the solvent, **7a** was isolated as a bright yellow powder (38.0 mg, 48%). ^1H NMR ($CDCl_3$, δ): 3.02 (br, s, CH), 2.53 (s, CH). $^{11}B(^1H)$ NMR (d_6-acetone, δ): −0.8, (1 B), −4.6 (1 B), −6.4 (3 B), −11.7 (2 B), −15.5 (1 B), −17.0 (1 B). $^{13}C(^1H)$ NMR (d_6-acetone, δ): 189.8, 189.3, 46.4, 44.0. IR (neat): 2586.1, 2556.0, 2541.1 (ν_{B-H}), 2081.1 ($\nu_{C=O}$), 2018.2 ($\nu_{C=O}$), 1772.4 cm^{-1} ($\nu_{N=O}$). TLC (10% CH_2Cl_2 in hexanes): $R_f = 0.32$. HPLC t_R = 6.8 min (method B). HRMS (CI^-) m/z for $C_4H_{11}NO_3B_9Re$: calcd 405.1257, obsd 405.1150 [M^+].

Preparation of [2,2-$(CO)_2$-2-(NO)-8-(Ph)-2,1,8-*closo*-$ReC_2B_9H_{10}$] (8a). The rhenacarborane [Cs][**3a**] (269 mg, 0.440 mmol) was dissolved in a mixture of CH_3CN (15 mL) and H_2O (5 mL), forming a clear colorless solution. Aqueous solutions of $NaNO_2$ (0.50 mL, 34.5 mg, 0.500 mmol) and H_2SO_4 (2.0 M, 0.30 mL, 0.60 mmol) were added to the reaction mixture, which immediately became pale yellow. After 35 min, additional portions of $NaNO_2$ (0.30 mL,

(26) Causey, P. W.; Besanger, T. R.; Schaffer, P.; Valliant, J. F. *Inorg. Chem.* **2008**, *48*, 8213–8221.

20.7 mg, 0.300 mmol) and H_2SO_4 (2.0 M, 0.30 mL, 0.60 mmol) were added to the bright yellow solution. After an additional 90 min, the reaction mixture was transferred to a separatory funnel containing CH_2Cl_2 (30 mL) and H_2O (30 mL). The organic phase was collected and washed with H_2O (1 × 30 mL) and dried over Na_2SO_4 prior to removal of the solvent by rotary evaporation. The bright yellow residue was purified by automated reverse phase silica gel chromatography using a gradient of 60−100% CH_3CN vs H_2O. Compound **8a** was isolated as a bright yellow powder (183 mg, 87%). ^{1}H NMR (CD_2Cl_2, δ): 7.50 (m, 2 H, Ph), 7.26 (m, 3 H, Ph), 2.74 (s, CH). ^{11}B(^{1}H) NMR (CD_2Cl_2, δ): 2.0, (1 B), −3.5 (2 B), −6.0 (1 B), −6.7 (1 B), −10.1 (1 B), −11.1 (1 B), −15.3 (2 B). ^{13}C(^{1}H) NMR (CD_2Cl_2, δ): 189.1, 188.7, 139.8, 128.7, 67.7, 42.5. IR (neat): 2585.1 (br, ν_{B-H}), 2085.1 ($\nu_{C=O}$), 2026.6 ($\nu_{C=O}$), 1776.0 cm^{-1} ($\nu_{N=O}$). TLC (10% CH_2Cl_2 in hexanes): R_f = 0.22. HPLC t_R = 9.6 min (method B). HRMS (CI^-) *m/z* for $C_{10}H_{15}NO_3B_9Re$: calcd 483.1447, obsd 483.1478 [M^+]. X-ray quality single crystals were obtained from a solution of **8a** in CH_3CN/H_2O.

Preparation of [2,2-(CO)$_2$-2-(NO)-1,8-(Bn)$_2$-2,1,8-*closo*-ReC$_2$B$_9$H$_9$] (9a). Compound [Cs][**4a**] (238.7 mg, 0.333 mmol) was dissolved in a mixture of CH_3CN (15 mL) and H_2O (5 mL), yielding a clear colorless solution. Solutions of aqueous $NaNO_2$ (0.90 mL, 28.4 mg, 0.412 mmol) and H_2SO_4 (2.0 M, 0.25 mL, 0.50 mmol) were added to the reaction mixture, which became yellow within 5 min. After stirring for 2 h, additional portions of aqueous $NaNO_2$ (1.00 mL, 13.7 mg, 0.199 mmol) and H_2SO_4 (2.0 M, 0.10 mL, 0.20 mmol) were added. The bright yellow solution was stirred an additional 18 h. The product was extracted into CH_2Cl_2 (50 mL) and washed with H_2O (25 mL). The organic phase was dried over Na_2SO_4 prior to removal of the solvent by rotary evaporation. The dark yellow residue was purified by automated reverse phase silica gel chromatography using a gradient of 60−100% CH_3CN vs H_2O. Compound **9a** was isolated as a yellow oil (166.1 mg, 85%). ^{1}H NMR ($CDCl_3$, δ): 7.36−7.28 (m, 6 H, C_6H_5), 7.18 (m, 2 H, C_6H_5), 7.02 (d, 2 H, C_6H_5), 3.26 (s, 2 H, C*H*$_2$-Ph), 3.12 (s, 2 H, C*H*$_2$-Ph). ^{11}B(^{1}H) NMR ($CDCl_3$, δ): 2.3 (1 B), −2.2 (1 B), −4.5 (2 B), −5.5 (1 B), −6.8 (1 B), −10.3 (2 B), −12.4 (1 B). ^{13}C(^{1}H) NMR ($CDCl_3$, δ): 188.6 (CO), 187.7 (CO), 139.5, 137.7, 130.2, 130.2, 129.6, 128.6, 128.4, 128.0, 127.4 (C_{Ar}), 74.5 (br), 66.1 (br), 48.6, 46.7. IR (neat): 2572.1 (br, ν_{B-H}), 2082.7 ($\nu_{C=O}$), 2026.5 ($\nu_{C=O}$), 1763.6 cm^{-1} ($\nu_{N=O}$). TLC (20% CH_2Cl_2 in hexanes): R_f = 0.37. HPLC t_R = 15.2 min (method B). HRMS (CI^+) *m/z* for $C_{18}H_{23}NO_3B_9Re$: calcd 587.2073, obsd 587.2043 [M^+].

Radiochemistry. *Caution:* ^{99m}Tc is a γ-emitter (E_γ = 140 keV, $t_{1/2}$ = 6 h), while the radioactive rhenium isotopes ^{186}Re ($E_{max\beta}$ = 1.07 MeV, $t_{1/2}$ = 3.8 d) and ^{188}Re ($E_{max\beta}$ = 2.12 MeV, $t_{1/2}$ = 17 h) are both β^- emitters. These isotopes should be used only in a licensed and appropriately shielded facility.

Preparation of Metallacarboranes 1b−4b. In a typical experiment, [^{99m}Tc(CO)$_3$(H$_2$O)$_3$]$^+$ (0.5 mL, 300 MBq) was added to a solution of [Na][*nido*-RR′C$_2$B$_9$H$_9$] (0.5 mL, 20 mM) in aqueous ethanol (10% v/v, 1 mL) under an inert (argon) atmosphere. The reaction mixture was heated in a microwave reactor for 5 min at 180 °C. The resulting solution was loaded onto a C18 solid phase extraction cartridge, which was flushed with H_2O (10 mL); the product was then eluted with CH_3CN (5 mL). Isolated radiochemical yields: **1b**, 60%; **2b**, 55%; **3b**, 65%; **4b**, 32%. Radio-HPLC retention times of **1b−4b** (HPLC method A, 21−23 min) were consistent with the UV-HPLC retention times of the corresponding rhenium complexes **1a−4a**.

Preparation of Nitrosated Metallacarboranes 6b, 8b, and 9b. The following general procedure was used: solid $NaNO_2$ (10 mg, 6.9 mmol) was added to a solution of **1b−4b** (1.5 mL, 75 MBq) in CH_3CN followed immediately by aqueous H_2SO_4 (2 M, 3 drops). After 5 min, the reaction mixture was loaded onto a C18 solid phase extraction cartridge, which was flushed with CH_3CN/H_2O (1:1, 5 mL); the product was eluted with CH_3CN (4 mL). Isolated radiochemical yields: **6b**, 64%; **8b**, 79%; **9b**, 62%. Radio-HPLC retention times of **6b**, **8b**, and **9b** (HPLC method B, 8−18 min) were consistent with the UV-HPLC retention times of the corresponding rhenium complexes **6a**, **8a**, and **9a**.

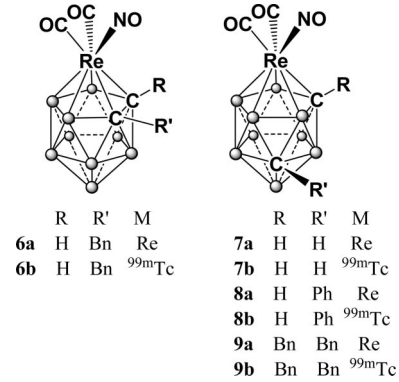

Figure 2. Novel 3,1,2- (left) and 2,1,8-dicarbonylnitroso-*closo*-rhenacarboranes (right). Shaded circles represent BH units.

Preparation of the Rhenacarborane $^{186/188}$Re-8a. A 1:1 mixture of [$^{186/188}$Re(CO)$_3$(H$_2$O)$_3$]$^+$ and [$^{186/188}$ReO$_4$]$^-$ (1.2 mL, 18.3 MBq) at pH 7 was added to a solution of [Na][1-Ph-*nido*-C$_2$B$_9$H$_{11}$] (0.5 mL, 22 mM) under an inert (argon) atmosphere. The reaction mixture was heated in a microwave reactor for 5 min at 200 °C. The resulting solution was loaded onto a C18 solid phase extraction cartridge, which was flushed with H_2O (10 mL); the radioactive rhenacarborane **$^{186/188}$Re-3a** was then eluted with CH_3OH (2.5 mL) and identified by radio-HPLC (method A, t_R = 22.8 min). A solution of **$^{186/188}$Re-3a** (0.9 mL, 0.96 MBq) was treated with $NaNO_2$ (6.5 mg, 94 μmol) and aqueous H_2SO_4 (0.2 mL, 2 M); after 5 min the reaction mixture was loaded onto a C18 solid phase extraction cartridge, which was flushed with aqueous CH_3CN (6 mL, 60%); the product **$^{186/188}$Re-8a** was then eluted with neat CH_3CN (3 mL) and identified by radio-HPLC (method B, t_R = 9.7 min). Isolated yield: 0.36 MBq, 38%.

X-ray Crystallography. A yellow plate-like crystal of **8a** (0.3 mm × 0.18 mm × 0.002 mm) was mounted on a glass fiber using epoxy. Data were collected on a Bruker Smart APEX2 diffractometer equipped with a three-circle D8 goniometer using graphite-monochromated Mo Kα radiation (phi and omega scans). The programs APEX2[27] and SAINT[28] were used for data collection and refinement; data reduction was carried out using the SAINT software program.[28] A numerical absorption correction was applied using XPREP[29] face indexing. Crystallographic data are summarized in Table 1. The structure was solved by direct methods and refined by full matrix least-squares using the Bruker SHELXTL program library.[30] Some hydrogen atoms were located from the difference map; the remainder were included at geometrically idealized positions. Non-hydrogen atoms were refined anisotropically. Thermal ellipsoid plots were created using Mercury 1.4.1.[31]

Results and Discussion

Synthesis and Characterization of Nitrosated Rhenacarboranes 6a−9a. We had previously reported a general synthetic route (Figure 1) to carborane complexes of the [Re(CO)$_3$]$^+$ core using a microwave reactor to decrease reaction times.[14,15] The metallacarboranes were prepared as sodium salts due to the presence of excess NaF from the degradation of the parent *closo*-carboranes to the more reactive *nido*-species. The products were isolated as oils following silica gel chromatography. In addition

(27) *M86-Exx078 APEX2 User Manual*; Bruker AXS Inc.: Madison, WI, 2006.

(28) Sheldrick, G. M. *SAINT, Release 6.45*; Siemens Energy and Automation Inc.: Madison, WI, 2003.

Table 1. Crystallographic Data for Compound 8a

empirical formula	$C_{10}H_{15}B_9NO_3Re$
fw	480.74
space group	*P*2(1)/*c*
a, Å	8.0428(9)
b, Å	7.0814(8)
c, Å	29.3210(3)
α, deg	90
β, deg	96.073(2)
γ, deg	90
V, Å^3	1660.6(3)
Z	4
T, K	296(2)
λ, Å	0.71073
d_{calc}, g cm^{-3}	1.923
μ, mm^{-1}	7.323
F(000)	904
R^a	0.026
$R_w{}^b$	0.040

^{a} $R = [\sum||F_o| - |F_c||]/[\sum|F_o|]$ for reflections with $I > 2.00\sigma(I)$. ^{b} $R_w = ([\sum w(F_o^2 - F_c^2)^2]/[\sum w(F_o^2)^2])^{1/2}$ for all reflections.

to the inconvenience of working with oils, the presence of residual methanol in the lattice was problematic for our current aims due to its reactivity toward the nitrosonium $[NO]^+$ cation. As a consequence, the synthesis of rhenacarboranes **1a**−**4a** was repeated, replacing the NaF with CsF and isolating the complexes by liquid−liquid (CH_2Cl_2/H_2O) extraction. From these reactions, the cesium salts of **1a**−**4a** were obtained in excellent yields (∼90%) as dry powders; spectroscopic data were consistent with those reported previously for the sodium salts.

The nitrosated rhenacarborane **5** was reportedly isolated following treatment of the corresponding rhenium tricarbonyl carborane [Cs][3,3,3-$(CO)_3$-*closo*-3,1,2-$ReC_2B_9H_{11}$], a cage isomer of **1a**, with several portions of $[NO][BF_4]$ at −60 °C under strictly anhydrous conditions.[16,32] The nitrosonium cation "$[NO]^+$" was substituted in place of a single CO unit and renders the formerly monoanionic metallacarborane charge-neutral. When analogous reactions with the related rhenacarboranes **1a**−**4a** were undertaken, the expected mononitroso species **6a**−**9a** (Figure 2), respectively, were obtained in modest (∼30%) yields. Though a viable means of generating the target species, this method is not suited for radiopharmaceutical applications due to the exacting reaction conditions and dry organic solvents that are required.

Toward aqueous syntheses of the metallacarboranes **1a**−**4a**, sodium nitrite was selected as the nitrosating agent of choice for our purposes due to its stability in aqueous media; the nitrosonium cation is formed *in situ* via the HNO_2 intermediate.[25] Optimization of the reaction conditions was facilitated by the substantial increase in the TLC retention factor (R_f) values of the neutral NO-containing analogues **6a**−**9a** as compared to their anionic precursors **1a**−**4a**, which provided a convenient means of monitoring the reaction progress. In contrast to the 4 molar equiv of "$[NO]^+$" and moderately acidic (∼1 M) media employed for the nitrosation of *fac*-$[Re(CO)_3Br_3]^-$,[25] a slight excess of $NaNO_2$ combined with a minimal amount of H_2SO_4 (2 molar equiv) was ultimately determined to be an efficient route to **6a**−**9a**, while eliminating the formation of unwanted oxidized species. An alternate synthetic approach of generating the target rhenacarborane complexes via the reaction of the $[Re(CO)_2(NO)]^{2+}$ core with *nido*-carboranes was not successful.

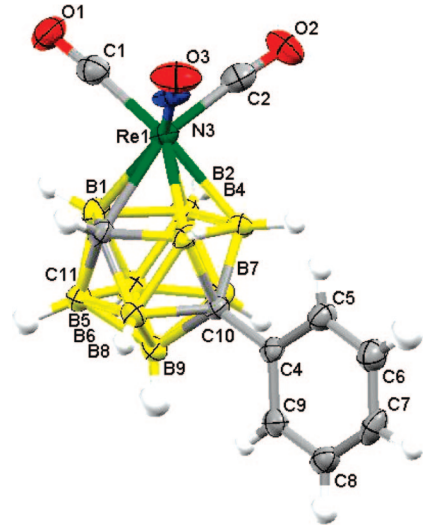

Figure 3. Thermal ellipsoid plot of **8a** (50% probability ellipsoids).

Table 2. Selected Bond Lengths (Å) and Angles (deg) for 8a

O(1)−C(1)	1.159(5)	O(2)−C(2)	1.161(5)
O(2)−N(3)	1.174(5)	Re(1)−B(1)	2.332(5)
Re(1)−B(2)	2.345(6)	Re(1)−B(3)	2.309(5)
Re(1)−B(4)	2.276(5)	Re(1)−C(11)	2.306(4)
B(5)−B(9)	1.754(8)	B(6)−B(9)	1.769(8)
B(7)−B(9)	1.782(7)	B(8)−B(9)	1.752(8)
C(10)−B(9)	1.737(6)	C(4)−C(10)	1.510(6)
B(1)−Re(1)−B(2)	45.1(2)	B(1)−Re(1)−B(3)	77.4(2)
B(1)−Re(1)−B(4)	77.60(18)	B(1)−Re(1)−C(11)	44.41(17)
B(5)−B(9)−C(10)	105.3(3)	B(6)−B(9)−C(10)	105.9(3)

The nitrosated rhenacarboranes **6a**−**9a**, which are bright yellow in color, were characterized spectroscopically. Notably, each infrared spectrum contained a strong *ν*(N═O) stretching absorption at ∼1773 cm^{-1} along with sharp *ν*(C═O) absorptions at ∼2082 and ∼2020 cm^{-1} and broad BH stretching vibrations centered near 2585 cm^{-1}. The ^{1}H and ^{13}C NMR spectra exhibited the expected resonances for the single Bn or Ph substituents of **6a** and **8a**, respectively, with the carborane cage C*H* unit giving rise to a broad ^{1}H singlet at 2.56 ppm (**6a**) or 2.74 ppm (**8a**). Two distinct sets of benzyl resonances were present in the ^{1}H and ^{13}C NMR spectra of **9a** due to the symmetry inequivalence of the two groups; similarly, the CH vertices in the 1 and 8 cage positions of **7a** resonated at 3.02/2.53 ppm and 46.4/44.0 ppm in the ^{1}H and ^{13}C NMR spectra, respectively. The ^{13}C NMR spectra of all four derivatives **6a**−**9a** displayed an additional two signals near 189 ppm due to the two symmetry inequivalent CO units. The ^{11}B(^{1}H) NMR spectra were complex, as is typical for metallacarboranes,[33] but displayed the same peak patterns seen for the precursors **1a**−**4a**.[14,15] The slight increase (+7 ppm) in the chemical shift values reflected the decreased electron density in the carborane cage in the neutral rhenacarboranes **6a**−**9a**. High-resolution mass spectrometry was used to confirm the formulation of the products, with the characteristic complex isotope pattern due to the presence of nine boron atoms (^{10}B, 19.9%; ^{11}B, 80.1%) and one rhenium atom (^{185}Re, 37.4%; ^{187}Re, 62.6%) observed centered at the expected $[M]^+$ values. The purity of the complexes was established as >95% by HPLC.

The solid state structure of **8a** was confirmed by single-crystal X-ray diffraction (Table 1). The crystallographic data showed

(29) Sheldrick, G. M. *XPREP Release 6.45*; Siemens Energy and Automation Inc.: Madison, WI, 2003.
(30) Sheldrick, G. M. *SHELXTL, Release 6.14*; Siemens Crystallographic Research Systems: Madison, WI, 2000.
(31) *Mercury 1.4.1*; CCDC, 2001−2005.
(32) Orlando, J. H.; Jelliss, P. A. Personal communication to the authors, 2006.
(33) See, for example: (a) Buehl, M.; Holub, J.; Hnyk, D.; Machacek, J. *Organometallics* **2006**, *25* (9), 2173–2181. (b) Hughes, A. K. *J. Organomet. Chem.* **2002**, *657* (1−2), 9–19. (c) Fox, M. A.; Howard, J. A. K.; Hughes, A. K.; Malget, J. M.; Yufit, D. S. *J. Chem. Soc., Dalton Trans.* **2001**, *15*, 2263–2269.

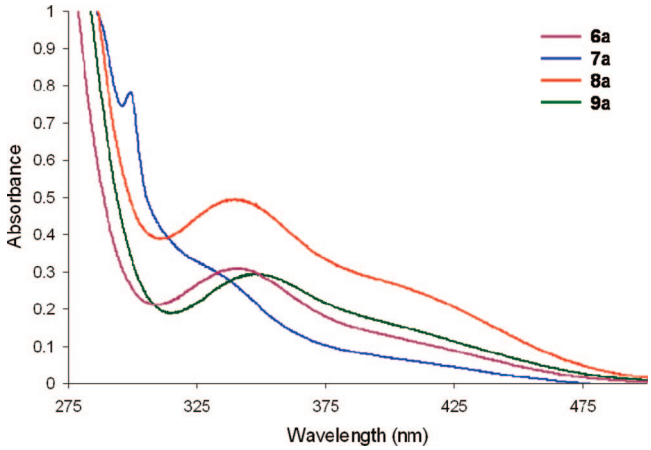

Figure 4. Absorbance spectra of **6a**−**9a** in CH_3CN (250−500 nm).

Table 3. Absorbance and Emission Characteristics of 5 and 6a−9a

parameter	5[a]	6a	7a	8a	9a
λ_{max}, nm	355	341	300	340	348
ε, M^{-1} cm^{-1}	500	619	1580	993	584
excitation wavelength, nm	285	341; 400	300; 340	340; 410	348; 405
emission wavelength, nm	435	398; 460	313; 402	392; 463	411; 471

[a] Data taken from ref 18.

the expected ReC_2B_9 icosahedron (Figure 3), slightly distorted at the Re vertex due to the larger size of rhenium as compared to boron and carbon. See Table 2 for pertinent bond lengths and angles. The average Re−B bond distance in **8a** (2.316(5) Å) was consistent with those in the related monoanionic rhenacarborane [Na][2,2,2-$(CO)_3$-8-(4-OH-C_6H_4)-*closo*-$ReC_2B_9B_{10}$] (2.30 Å)[14] and the neutral zwitterionic complex (2,2,2-$(CO)_3$-8-[(*N*-Me)$CH_2C_5H_4N$]-2,1,8-*closo*-$ReC_2B_9H_{10}$) (2.32 Å).[15] Due to the 3-part disorder between C(1), C(2), and N(1), a discussion of the metrical parameters pertaining to the CO and NO units is not appropriate, although in all cases the ReEO (E = C, N) angle was near linear (176.1(4)°).

Absorption and Emission Properties of Rhenacarboranes 6a−9a. As stated previously, compounds **6a**−**9a** are a distinctive yellow color both in the solid state and in solution. This is explained by their absorbance spectra (Figure 4): all display absorbances at the lower end of the visible range and into the UV region with molar extinction coefficients (Table 3) ranging from 584 M^{-1} cm^{-1} (**9a**) to 1580 M^{-1} cm^{-1} (**7a**). In addition to a large absorbance at ∼250 nm, a local maximum was observed for each of **6a**−**9a** at 300−348 nm (see Table 3). A comparison of the data for **7a** with those reported elsewhere[17,18] for its cage isomer **5** revealed the impact of altering the carborane cage configuration from 3,1,2 (**5**) to 2,1,8 (**7a**): the local absorption maximum of **7a** (λ_{max} = 300 nm; ε = 1578 cm^{-1} M^{-1}) is more intense and significantly blue-shifted relative to that of **5** (λ_{max} = 355 nm; ε = 500 cm^{-1} M^{-1}). The lone 3,1,2 isomer **6a** and the remaining 2,1,8 cage isomers **8a** and **9a**, both of which bear organic substituents attached to the carborane cage, showed absorption λ_{max} values more similar to that of **5**. The additional conjugation of the phenyl ring in **8a** resulted in a red-shift of the λ_{max} compared to the unsubstituted **7a**. The λ_{max} observed for the benzyl-substituted complexes, **6a** and **8a**, were also red-shifted, suggesting secondary effects of the substituents on the cage-centered absorption.

Excitation of solutions of **6a**−**9a** at ∼250 nm did not produce substantial fluorescence; however, upon increasing the excitation wavelength, fluorescence was observed for all four compounds. In the case of **7a**, excitation at 300 nm resulted in fluorescence at 313 nm; at 340 nm, emission at 402 nm was revealed upon correction for solvent contributions (Figure 5). The monophenyl species **8a** exhibited emission at 392 nm upon excitation at 340 nm, while very weak fluorescence occurred (463 nm emission maximum) upon irradiation at 410 nm. The emission maxima for the benzyl-containing carboranes **6a** and **9a** were 398 and 411 nm, respectively, when excited at ∼340 nm; very weak fluorescence was also detected following excitation at 400 nm (**6a**) or 405 nm (**9a**). The substituents on the carborane cage appear to have a large effect on the fluorescent properties of the complexes. The nature of the other chelating ligands may also affect emission properties but were not investigated in our work. While the fluorescence spectra of **6a**−**9a** were not greatly affected by the presence of atmospheric oxygen, slight reductions in fluorescence intensities were observed in air-equilibrated samples as compared to those prepared under a nitrogen atmosphere for **7a** and **8a**.

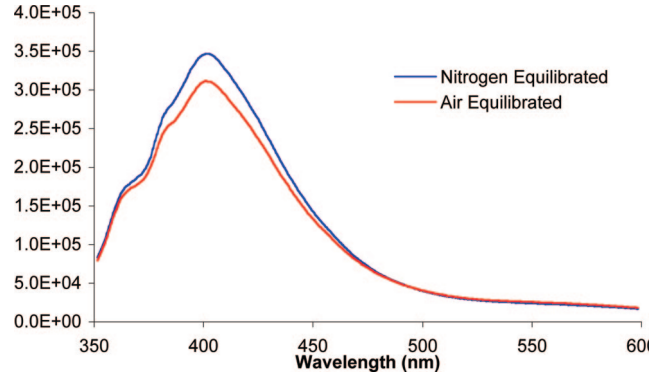

Figure 5. Fluorescence emission spectra of **7a** following excitation at 340 nm.

Quantum yields and fluorescence lifetime measurements were attempted for compounds **6a**−**9a**; however, it was possible to obtain reliable data only for **7a** due to the extremely weak fluorescence for the other compounds. Although the quantum yield for **7a** was modest (0.002), it is comparable to those of the single amino acid chelate complexes that have been successfully imaged *in vitro* using fluorescence microscopy.[4,5] The average fluorescence lifetime of **7a** was determined to be 8.1 ns; slightly more rapid fluorescence decay was seen for air-equilibrated samples than for those equilibrated under a nitrogen atmosphere (due to the presence of quenching species (oxygen) in the solution). The observed lifetimes are comparable to organic fluorophores, suggesting that the fluorescence is due to cage-centered electronic transitions and not metal-to-ligand charge transfer. Because of the short lifetimes, both the fluorescence intensity and lifetime measurements show minimal sensitivity to the presence of oxygen.

The data presented here indicate that despite the inherently weak nature of the fluorescence of these organometallic complexes, altering the electronic nature of the appended functional group(s) can potentially be used to tune the quantum efficiency and other key fluorescence properties of this class of molecules. The photophysical profiles of these carborane-based agents are significantly different that those of the bifunctional chelate complexes of Re(I) presented elsewhere.[4,5] Further investigation is needed to better understand the fundamental basis for the observed differences in fluorescence properties.

Radiosynthesis and Nitrosation of 1b−4b. With the rhenacarboranes **1a**−**4a** and **6a**−**9a** in hand, the corresponding *nido-ortho*-carborane ligands were reacted with $[^{99m}Tc(CO)_3]^+$ at 180 °C in a microwave reactor. Radio-HPLC (method A) indicated complete consumption of the technetium-99m reagent (t_R = 3.5 min) and excellent conversion of the radioactivity to technetacarboranes **1b**−**4b** after only 5 min. The sole byproduct of the reactions was identified as $[^{99m}TcO_4]^-$ (t_R = 11.0 min), formed

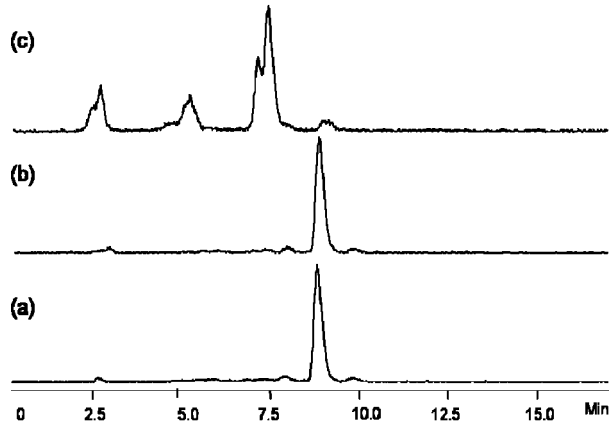

Figure 6. Radio-HPLC chromatograms of **8b** (method B): (a) at $t = 0$; (b) at $t = 5$ h in CH_3CN; (c) at $t = 3.5$ h in H_2O/CH_3CN.

via reoxidation of the $[^{99m}Tc(CO)_3(H_2O)_3]^+$ starting material. Following removal of residual salts by a convenient solid phase extraction method, the radiometallacarboranes were isolated in good (32−65%) yields.

The reactivities of **1b**−**4b** toward different sources of nitrosonium ion[25]—$[NO][BF_4]$, $[NO][HSO_4]$, and $NaNO_2$—were explored; the replacement of one CO unit was found to occur instantaneously upon addition of any of these reagents. Each reaction was quenched by loading onto a solid phase extraction cartridge and flushing with water to remove the excess $[NO]^+$. The nitrosated radiometallacarborane was then eluted from the cartridge using neat acetonitrile and identified by correlation of the radio-HPLC retention time (method B) with the UV-HPLC retention time of the corresponding rhenacarborane. Compounds **6b**, **8b**, and **9b** were successfully isolated in good yields (62−79%) in this fashion, but surprisingly, formation of complex **7b** was not observed.

An examination of the stability of **6b**, **8b**, and **9b** in solution yielded unexpected results. While the radiochemical purity of the products was not affected by allowing the products to stand in acetonitrile for several hours, metallacarboranes **6b** and **8b** were found to degrade completely to a mixture of species within 1 and 4 h, respectively, in aqueous media (Figure 6). These results, which contrast the stability of the rhenium analogues (*vide infra*), suggested a possible reason for the repeated failure of attempts to isolate **7b**: this complex may simply undergo rapid hydrolysis before HPLC data can be obtained.

In sharp contrast to the monobenzyl derivative **6b**, the dibenzylcarborane derivative **9d** remained intact for the duration of the stability study (>4 h). More surprising yet was the apparent decomposition of **8b** when we have recently demonstrated that [2,2-$(CO)_3$-2-(NO)-8-(4-OH-C_6H_4)-*closo*-$^{99m}TcC_2B_9B_{10}$],[34] which differs from **8b** only in the addition of a hydroxyl group at the *para* position of the phenyl ring, is stable (>18 h) in water. It is apparent from these disparate results that both steric and electronic factors influence the stability of this class of compounds.

Although complexes of the $[Re(CO)_2(NO)]^{2+}$ core are known to be more reactive in water than species containing $[Re(CO)_3]^+$,[35,36] aqueous solutions of **6a**−**9a** remained unaffected after several weeks in contrast to their ^{99m}Tc analogues, calling into question whether the process observed for **6b**/**8b** was caused by a reaction such as hydrolysis at the metal core or whether it was due to radiolysis or an underlying difference between the reactivities of the two metals. To probe this, radioactive rhenium was used to prepare the $^{186/188}Re$ analogue of **8a**; as both are beta-emitters, radiolysis should be more prevalent for these two isotopes than for the primarily gamma-emitting technetium-99m at comparable activities and concentrations. Radio-HPLC indicated that **$^{186/188}$Re-8a** undergoes an analogous process to **8b** albeit at a much slower rate (∼75% decomposition in 22 h), a rare example of a radioactive rhenium complex being more stable than its ^{99m}Tc analogue. From this, it was concluded that the decomposition of **$^{186/188}$Re-8a** and **8b**, but not **8a**, occurs via a hitherto unknown process that is greatly accelerated at the tracer level. The differing specific activity of the products and oxidation potentials of the two metals likely play key roles in the disparity between the reaction rates of **$^{186/188}$Re-8a** and **8b**.

At present, the identities of the decomposition products remain uncertain, though preliminary carrier-added experiments incorporating small amounts of carrier ^{99}Tc ($t_{1/2} = 2.1 \times 10^5$ years) into syntheses of the ^{99m}Tc-technetacarboranes **6b** and **9b** have been attempted to elucidate the reaction pathway. Following complete radioactive decay of the ^{99m}Tc (1 week), samples analyzed by mass spectrometry indicated that the technetium-carborane unit had remained intact, adding further weight to the supposition that the reaction with water occurs at the $[^{99m}Tc(CO)_2(NO)]$ core, rather than loss of the carborane cage.

Conclusions

An aqueous synthesis of dicarbonyl nitroso rhenacarboranes has been developed, and their luminescence properties have been examined and found to be suitable for *in vitro* imaging. The corresponding ^{99m}Tc-carborane complexes were generated from commercially available $[^{99m}TcO_4]^-$ in less than 2 h. Certain of these species are prone to decomposition in water; at present, no correlation can be made between the rate of reaction and the carborane cage configuration or steric crowding at the metal center. Further study is necessary in order for the aqueous stability of a given $[^{99m}Tc(CO)_2(NO)]$-carborane to be accurately predicted prior to its synthesis. With this established, future work will focus on preparing metallacarboranes (M = ^{99m}Tc, Re) bearing a biological vector as targeted molecular imaging probes.

Acknowledgment. We thank NSERC (Canada) for funding this research and for a fellowship (A.F.A.), Dr. R. H. Tomlinson (McMaster Nuclear Reactor) for providing samples of $[^{186/188}ReO_4]^-$, Drs. J. Britten and H. Jenkins for collecting and solving the X-ray data, and Drs. P. Jelliss and J. Orlando (St. Louis University) for helpful information regarding the preparation of compound **5**.

Supporting Information Available: The crystallographic CIF file for compound **8a** and additional fluorescence data are included as Supporting Information and is available free of charge via the Internet at http://pubs.acs.org.

OM8011807

(34) Causey, P. W.; Besanger, T. R.; Valliant, J. F. *J. Med. Chem.* **2008**, *51* (9), 2833–2844.
(35) Lehaire, M.-L.; Grundler, P. V.; Steinhauser, S.; Marti, N.; Helm, L.; Hegetschweiler, K.; Schibli, R.; Merbach, A. E. *Inorg. Chem.* **2006**, *45* (10), 4199–4204.
(36) Kurz, P.; Rattat, D.; Angst, A.; Schmalle, H.; Spingler, B.; Alberto, R.; Berke, H.; Beck, W. *Dalton Trans.* **2005**, 804–810.